Title

Bringing Plant Immunity to Light: A Genetically Encoded, Bioluminescent Reporter of Pattern Triggered Immunity in *Nicotiana benthamiana*

Authors

Anthony G. K. Garcia[1], Adam D. Steinbrenner[1]*

[1]Department of Biology, University of Washington, Seattle WA 98195 U.S.A.

*Corresponding author: A. D. Steinbrenner; E-mail: astein10@uw.edu

Keywords: *Agrobacterium tumefaciens,* bioluminescence, *Nicotiana benthamiana,* pattern recognition receptor, pattern triggered immunity, receptor-like proteins

Funding: National Science Foundation Grant number: IOS-2139986, The Mary Gates Endowment for Students

Abstract

Plants rely on innate immune systems to defend against a wide variety of biotic attackers. Key components of innate immunity include cell-surface pattern recognition receptors (PRRs), which recognize pest/pathogen-associated molecular patterns (PAMPs). Unlike other classes of receptors which often have visible cell death immune outputs upon activation, PRRs generally lack rapid methods for assessing function. Here, we describe a genetically encoded bioluminescent reporter of immune activation by heterologously-expressed PRRs in the model organism *Nicotiana benthamiana*. We characterized *N. benthamiana* transcriptome changes in response to *Agrobacterium tumefaciens (Agrobacterium)* and subsequent PAMP treatment to identify PTI-associated marker genes, which were then used to generate promoter-luciferase fusion fungal bioluminescence pathway (FBP) constructs. A reporter construct termed *pFBP_2xNbLYS1::LUZ* allows for robust detection of PTI activation by heterologously expressed PRRs. Consistent with known PTI signaling pathways, activation by receptor-like protein (RLP) PRRs is dependent on the known adaptor of RLP PRRs, SOBIR1. This system minimizes the amount of labor, reagents, and time needed to assay function of PRRs and displays robust sensitivity at biologically relevant PAMP concentrations, making it ideal for high throughput screens. The tools described in this paper will be powerful for studying PRR function and investigations to characterize the structure-function of plant cell surface receptors.

Introduction

Plants perceive pests and pathogens through cell surface-localized immune receptors, termed pattern recognition receptors (PRRs). Canonically, these transmembrane proteins activate pattern triggered immunity (PTI) in response to conserved pathogen associated molecular patterns (PAMPs) (Boutrot & Zipfel, 2017). PTI consists of a suite of defense signaling and outputs including reactive oxygen species (ROS) production, ethylene production, peroxidase upregulation, callose deposition, stomatal modifications, calcium oscillations, and phytohormone production (Aldon et al., 2018; Berens et al., 2017; Broekgaarden et al., 2015; Melotto et al., 2017; Mott et al., 2018; Qi et al., 2017; Toyota et al., 2018; Y. Wang et al., 2021). These outputs aid in transcriptional reprogramming to improve plant resistance against attackers (Denoux et al., 2008; Navarro et al., 2004). Understanding immune activation by PRRs is critical for developing novel strategies to improve plant resistance against pests and pathogens.

The model organism *Nicotiana benthamiana* represents a significant resource in the field of plant immunity, in part because of robust immune phenotypes conferred by transiently expressed intracellular plant immune receptors (Goodin et al., 2008; Buscaill et al., 2021). *Agrobacterium*-mediated transient transformation of *N. benthamiana* allows for rapid expression of proteins, which is particularly applicable for mutant screening and structure-function analysis. For example, screening cell death as a visual reporter triggered by NLR activation has allowed investigations of structural features of nucleotide-binding leucine-rich repeat (NLR) proteins (Segretin et al., 2014; Steinbrenner et al., 2015; Adachi et al., 2019).

Transient transformation of *N. benthamiana* similarly serves as a powerful tool for studying PRRs, but there is currently a lack of robust visual reporters of PRR function in

N. benthamiana analogous to cell death. Several cell surface immune receptors activate cell death phenotypes in other species, including leucine-rich repeat receptor-like proteins (LRR-RLPs) such as *Arabidopsis thaliana* RLP42 and *Solanum lycopersicum* Ve1, but these LRR-RLPs do not necessarily activate cell death upon heterologous expression in *N. benthamiana* or can require strong repeated elicitation (de Jonge et al., 2012; Z. Zhang et al., 2013; L. Zhang et al., 2014). Because heterologously expressed PRRs do not activate visual markers of PTI in *N. benthamiana,* immune responses mediated by transiently expressed PRRs are instead detected using early markers of PTI defense activation, including PAMP-induced ROS, ethylene, or peroxidase production (Mott et al., 2018; Steinbrenner et al., 2020). However, these assays are laborious or are hampered by the presence of *Agrobacterium* as a background source of PTI activation.

Reporters utilizing luminescence, fluorescence, or pigmentation have been adapted to study a variety of plant signaling processes (DeBlasio et al., 2010; Furuhata et al., 2020; He et al., 2020). However, no transiently expressed reporters of immune activation in intact *N. benthamiana* leaves have been described. A high sensitivity luciferase-based system for measuring pattern triggered immunity in protoplasts of *N. benthamiana* was previously reported (Nguyen et al., 2010), but was not tested for heterologously expressed PRRs and required external addition of luciferin. A different system using a bioluminescent strain of *Agrobacterium* expressing the bacterial *lux* operon allows for monitoring of *Agrobacterium* during transient transformation and quantification of effector triggered immunity (ETI), but has not yet been applied to PTI (Jutras et al., 2021). *N. benthamiana* lines stably expressing the fluorescent Ca2+ indicator GCaMP3

allow for detection of signaling in response to various biotic and abiotic stresses, including signaling activated by transiently expressed receptor-like kinases (DeFalco et al., 2017). However, stable expression of GCaMP3 limits the ability to quickly test different *N. benthamiana* genotypes and mutants lacking components of the signaling pathway. Finally, fluorescent proteins and pigments are simple to measure, but lack the same low background and high sensitivity of luciferase-based assays (Haugwitz et al., 2008; Thorne et al., 2010), which limits the ability to detect the range of responses that may occur in response to an immune elicitor.

To develop a generic PTI reporter, we performed transcriptomic analysis of *N. benthamiana* upon activation of a heterologously expressed PRR and adapted endogenous markers into a luciferase-based system that retains sensitivity but eliminates the need to introduce exogenous substrate. By encoding a metabolic pathway that allows for endogenous production of fungal luciferin alongside the fungal luciferase (*LUZ)* enzyme, the fungal bioluminescence pathway (FBP) system circumvents requirements for external addition of substrate while still remaining sensitive to subtle changes in gene expression (Khakhar et al., 2020; Mitiouchkina et al., 2020). Importantly, the features of the FBP system were well-suited for a reporter system that meets several criteria to be useful for studying plant cell surface immune receptors in a heterologous system: 1) highly sensitive to biologically relevant concentrations of immune elicitors, 2) capable of rapid, low cost, and visual assessment of immune activation, and 3) robust to low numbers of biological replicates and background immune elicitation by *Agrobacterium*. Therefore, we utilized the FBP

system to develop a reporter of immune activation by heterologously expressed cell surface receptors.

Materials and Methods

Plant Materials and Growth Conditions

N. benthamiana plants were transplanted one week after sowing and grown at 20°C under 12-hour light and dark cycles. The seedlings were grown under humidity domes for four weeks, after which the domes were removed, and the plants were grown an additional week before infiltrations. Fully expanded, mature leaves of six-week-old plants were used for all transient expression experiments.

Transcriptomic and qRT-PCR Analysis

For RNAseq analysis, an *N. benthamiana* stable transgenic line expressing *Phaseolus vulgaris* INR (INR-Pv 1-5) (Steinbrenner et al., 2020) was syringe infiltrated with Agrobacterium GV3101 (pMP90) at OD = 0.45 expressing empty vector (EV) pEarleyGate103 (Earley et al., 2006). 24 hpi, *Agrobacterium*-treated leaves were further infiltrated with H_2O or 1 μM In11 peptide and harvested after an additional 6 hpi. Total RNA was extracted using Nucleospin Plant RNA kit (#740949.250 Macherey-Nagel). RNA was used to generate Lexogen Quantseq 3' RNA seq libraries at Cornell University Institute of Biotechnology Genomics Facility. 3' reads were mapped to *N. benthamiana* genome v1.0.1 (Sol Genomics Network) using HISAT2 (Kim et al., 2019)

with options min-intronlen 60--max-intronlen 6000, counts by gene were analyzed using HTSeq-Count (Anders et al., 2015) with options -m intersection-nonempty --nonunique all, and differential expression was analyzed by DESeq2 (Love et al., 2014).

For qRT-PCR analysis, *N. benthamiana* plants were syringe infiltrated with *Agrobacterium* (OD600 .45) carrying either *p35s::PvINR* or pGreenII empty vector. 24 hours after infiltration, tissue was treated with either water or In11 and harvested after 6 hours. Total RNA was extracted using Trizol reagent (#15596018 Thermo Fisher Scientific, USA). cDNA libraries were generated using SuperScript IV Kit (#18090050 Thermo Fisher Scientific, USA). qRT-PCR reactions were conducted using Applied Biosystems PowerUp SYBR Green Master Mix (#A25742 Thermo Fisher Scientific, USA) and gene specific primer pairs (Supplementary Table S2). Changes in gene expression between water and In11 treatments were calculated using the ΔΔCq method, using ΔCq values normalized against *N. benthamiana EF1α* (D. Liu et al., 2012). Student's t-tests were performed between comparisons of *35s::PvINR* and EV treated tissue using the ggplot2 package in R (v4.1.2).

Generation of Reporter Constructs

Promoter regions of candidate marker genes were amplified from genomic DNA of *N. benthamiana* using primers designed against Niben v1.0.1 (Bombarely et al., 2012) with appended overhangs encoding either BsaI or BpiI restriction enzyme recognition sites (Supplementary Table S2). These primers amplified from the start codon to approximately 1.5 kb upstream. Promoter regions were then cloned into the Promoter + 5' untranslated region (UTR) acceptor backbone obtained from the Golden Gate MoClo

Plant Toolkit (Engler et al., 2014). Double promoter constructs were constructed by reamplifying the promoter region of interest with unique overhangs and cloning into the Level -1 universal acceptor backbones using the BsaI-HFv2 restriction enzyme (#R3733L New England Biolabs, USA). These parts were then assembled into the same Promoter + 5' UTR acceptor backbone using the BpiI restriction enzyme (#ER1012 Thermo Fisher Scientific, USA).

Reporter constructs were generated by first modifying the P307-FBP_6 constitutive autoluminescence construct previously described (Khakhar et al., 2020). P307-FBP_6 was a gift from Daniel Voytas (Addgene plasmid # 139697; http://n2t.net/addgene:139697; RRID:Addgene_139697). To simplify the process of cloning new reporter constructs with promoter regions of interest, the CaMV35s promoter originally used to drive *LUZ* was replaced with an insert encoding a blue-white selectable marker flanked by BsaI recognition sites supplying Promoter + 5' UTR MoClo overhangs (Supplementary Fig. S2A). This allows for simple, one-step assembly reactions. The promoter regions of interest were then cloned into this acceptor plasmid using the BsaI-HFv2 restriction enzyme. A template primer pair for amplification and cloning putative promoter regions directly into the pFBP_promoter_acceptor construct has been included (Supplementary Table S2).

Reporter constructs were transformed by electroporation into *Agrobacterium tumefaciens* GV3101 (pMP90). All sequences were verified by Sanger sequencing.

Agrobacterium-Mediated Transient Transformation and PAMP treatment

Agrobacterium strains carrying the constructs of interest were cultured in LB media containing kanamycin (50µg/mL), gentamicin (50µg/mL), rifampin (50µg/mL), and tetracycline (10ug/mL) for 24h. 3 mLs of culture were then pelleted and resuspended in infiltration media containing 10mM MES (pH 5.6), 10 mM MgCl2, and 150 µM acetosyringone. For coinfiltrations, separate strains harboring reporter and receptor constructs were combined at a final individual OD_{600} = 0.3 for a final cumulative OD_{600} =0.6. After 3h of incubation at room temperature (RT), the cell mixture was infiltrated into fully expanded leaves of 6-week-old *N. benthamiana* plants using a needless syringe.

To assess induction of luminescence, transformed regions were infiltrated with peptide 48 hours after *Agrobacterium* infiltration. Six hours after treatment, leaves were removed at the petiole and luminescence was immediately imaged using the Azure Imaging System with 8 seconds of exposure. Peptides were obtained from Genscript and diluted to specified concentrations in sterile autoclaved water.

Quantification and Statistical Analysis

Mean gray values of manually defined regions of interest were measured in ImageJ 1.53k. Average signal intensity (ASI) was determined by subtracting the average mean gray value of the untransformed background from the mean gray values of the regions of interest. Negative ASI indicates lower mean gray value than background. One-way ANOVAs and post-hoc Tukey's t-tests were conducted using the agricolae (v1.3-5) package in R (v4.1.2) and summarized as compact letter displays. Differing letters

represent statistically significant differences ($p<.05$) among pairwise comparisons. Figure editing and layouts were completed in Inkscape.

Phylogenetic Analysis

Using the annotated coding sequence of *Niben101Scf06684g03003.1*, a BLASTN search was conducted against the *Vigna unguiculata* (v1.2), *Phaseolus vulgaris* (v2.1), and *Arabidopsis thaliana* (TAIR10) genomes (predicted cDNA sequences). *Arabidopsis thaliana* was included to identify potential characterized homologs, and the two legume species were included as representative legume species that natively encode INR. After aligning the top 70 hits, a maximum likelihood phylogenetic tree was generated using FastTree. A subset of this tree was then selected and realigned as translated amino acid sequences using MAFFT (Katoh et al., 2019; Kuraku et al., 2013). A maximum likelihood tree was subsequently generated on the CIPRES web portal using RAXML-HPC2 on XSEDE (v8.2.12) (Miller et al., 2010; Stamatakis, 2014) with the automatic protein model assignment algorithm using maximum likelihood criterion and 100 bootstrap replicates. The resulting phylogeny was rooted and visualized using MEGA11 and edited in Inkscape.

Results

Differentially Expressed Genes in Response to Agrobacterium and PTI activation

Heterologous expression of PRRs in *N. benthamiana* allows for activation of PTI in response to cognate PAMPs, but transient expression requires introduction of *Agrobacterium*, a potentially independent source of PAMPs and activator of PTI responses. To characterize the transcriptional landscape of PTI induced by both *Agrobacterium* and individual PAMP treatment, we conducted transcriptomic analysis in plants stably expressing the *P. vulgaris* Inceptin Receptor (PvINR), an LRR-RLP which recognizes the peptide elicitor inceptin11 (In11) (Steinbrenner et al., 2020). Plants were infiltrated with *Agrobacterium* to mimic conditions during *Agrobacterium*-mediated transient transformation. After 24 hours, the *Agrobacterium*-infiltrated leaves were subsequently treated with water or In11 to induce immune signaling (Supplementary Fig. S1, “AH” or “AI”). Additionally, leaves previously mock infiltrated were infiltrated with water to account for effects of wounding during infiltration (Supplementary Fig. S1, “H”). Tissue was collected after 6 hours, and RNA sequencing was subsequently conducted to identify differentially expressed genes (DEGs) under each pair of conditions.

Compared to leaf tissue not previously infiltrated, infiltration with *Agrobacterium* affected expression of hundreds of genes (Fig. 1A, comparisons "AH vs H" and "AI vs H", Supplementary Table S1). A total of 1425 upregulated and 938 downregulated genes were significantly altered by *Agrobacterium* infiltration. The majority of DEGs were observed in both In11 and water treated tissue.

To identify useful markers of PTI activation in the context of *Agrobacterium*, we next compared gene expression in *Agrobacterium*-infiltrated leaf tissue in the presence or

absence of In11 peptide (AI vs AH). Only one gene was significantly differentially expressed (Supplementary Table S1, column “adj. p”). Since In11 treatment previously activated measurable early immune phenotypes (Steinbrenner et al., 2020), namely induced ROS and ethylene production, in identical experimental conditions, we reasoned that transcriptional changes at this timepoint may occur below the threshold for statistical significance. We therefore performed a separate analysis filtering for genes with $p<0.05$ differential expression by standard Wald test but without correction for multiple comparisons (Supplementary Fig. S1B, Supplementary Table S1, column “p-value”). With this relaxed threshold91 genes were characterized as upregulated by the addition of In11 (Supplementary Fig. S1). Interestingly, In11-upregulated genes overlapped with both *Agrobacterium*-upregulated (Supplementary Fig. S1B) and downregulated genes (Supplementary Fig. S1C), suggesting complex regulation of specific *N. benthamiana* PTI outputs.

We further filtered candidate PTI marker genes based on broad responsiveness to both *Agrobacterium* and In11. Nine genes showed higher Agrobacterium or In11 induced expression in all three comparisons (Fig. 1C, Supplementary Fig. S1B), suggesting a large dynamic range of gene expression able to be activated by both *Agrobacterium* PAMPs and by the addition of the separate individual PAMP, In11. To determine more confidently which of these genes are induced by In11 treatment, we conducted qRT-PCR analysis probing differences in expression of each of the candidate marker genes six hours after water and In11 treatment. We found that four genes showed significant induction after treatment with In11 in tissue transiently expressing *PvINR*, but not in tissue infiltrated with an empty vector strain: *Niben101Scf08566g08014*,

Niben101Scf04592g00020, *Niben101Scf06684g03003*, *Niben101Scf04652g00027* (Fig. 2). We conclude that these four genes serve as markers of INR-mediated responses to In11 in *Nicotiana benthamiana* after transient PRR expression. In summary, while the transcriptional effects of an additional PAMP, In11, 24 hours after Agrobacterium infiltration are subtle, candidate genes were observed with Agrobacterium and PAMP-inducible behavior consistent with broadly responsive marker genes.

An FBP Luminescence Reporter to Quantify Innate Immune Activation by PTI

To test whether the promoter regions of these genes could function in In11-inducible reporters, we generated promoter fusion constructs with promoter regions of the endogenous *N. benthamiana* marker genes driving expression of the fungal luciferase (LUZ). Original FBP constructs contain five genes of the pathway for both LUZ and substrate biosynthesis enzymes (Khakhar et al., 2020). We first generated an adaptable acceptor construct allowing MoClo-compatible cloning of promoters to drive LUZ expression (Supplementary Fig. 2A). This vector, *pFBP_promoter_acceptor*, is available on Addgene (confirmation pending). Using this construct, we replaced the original constitutive CaMV35S promoter originally driving LUZ with promoter regions of genes of Fig. 2. Of the two constructs we successfully generated, only a fusion driven by the promoter region of *Niben101Scf06684g03003* showed induction of luminescence upon In11 treatment in a PvINR-dependent manner (Fig. 3A, Supplementary Fig. S3). *Niben101Scf06684g03003* is a homolog of the *A. thaliana* Class III lysozyme *LYS1* (Supplementary Fig. S4) (X. Liu et al., 2014). We therefore termed this construct *pFBP_NbLYS1::LUZ* (hereafter *pLYS1::LUZ*). Importantly, infiltration damage during treatment with H_2O does not result in high background luminescence and is instead

287 comparable with tissue not infiltrated with the reporter (Supplementary Fig. S5A),
288 making luminescence upon induction with In11 easily detectable.

289 Luminescence induced by the *pLYS1::LUZ* construct was markedly lower than a
290 construct using the CaMV35S promoter to drive LUZ expression (Supplementary Fig.
291 S4B). However, duplication of promoters has been shown to effectively increase
292 strength of expression (Kay et al., 1987). To enhance the strength of reporter
293 expression and observable luminescence, we also constructed *pFBP_2xNbLYS1::LUZ*
294 (hereafter *p2xLYS1::LUZ*), a double promoter region construct where two copies of the
295 *NbLYS1* promoter were arranged adjacently and used to drive expression of luciferase
296 treatment (Supplementary Fig. S5B). When coexpressed alongside *PvINR*, the
297 *pLYS1::LUZ* single copy construct did not show a statistically significant difference in
298 luminescence between water and In11 treatment, while the *p2xLYS1::LUZ* double copy
299 construct did show a significant difference between the water and In11 treatments (Fig.
300 3A). We therefore elected to proceed using the *p2xLYS1::LUZ* FBP construct as a
301 reporter for all subsequent experiments.

302 Different assays for immune receptor function show varying degrees of sensitivity to low
303 elicitor concentrations (Mott et al., 2018). To determine the sensitivity of the FBP
304 reporter assay to In11 treatment, we coexpressed the *p2xLYS1::LUZ* reporter and
305 *p35s::PvINR* and conducted a dose-response experiment using increasing
306 concentrations of In11. We observed statistically significant differences in luminescence
307 between water and In11 treatments above 500 pM (Fig. 3B). This falls within the range
308 of reported In11 concentrations that are present in the oral secretions of caterpillars

during herbivory (Schmelz et al., 2006). As a result, the *p2xLYS1::LUZ* is a robust reporter of immune activation by biologically relevant elicitor concentrations.

Besides INR, other heterologously expressed PRRs are capable of conferring PTI immune signaling in *N. benthamiana* (Albert et al., 2015; Steinbrenner et al., 2020; L. Zhang et al., 2021). Furthermore, flg22 treatment induces expression of the *A. thaliana LYS1* homolog (X. Liu et al., 2014). To test whether the *p2xLYS1::LUZ* construct serves as a reporter of PRR activity more broadly, we also tested reporter inducibility by two cell surface PRRs from *A. thaliana*: EFR and RLP23. We observed background induction of luminescence in leaf tissue expressing EFR when treated with elf18 (Fig. 4C), potentially due to background induction of EFR by *Agrobacterium*. elf18 nonetheless robustly induces luminescence relative to mock treatment. We also observed induction of luminescence in leaf tissue expressing RLP23 when treated with nlp20 (Fig. 4D). Importantly, induction of luminescence is only observed in regions of interest where the cognate receptor-elicitor pair is present. Together, these data support the utility of the *p2xLYS1::LUZ* construct as a robust reporter of specific PRR-elicitor interactions.

SOBIR1 is necessary for INR-mediated Induction of Bioluminescence by Inceptin

Characterized LRR-RLPs are known to require the adaptor receptor-kinase SUPPRESSOR OF BIR1-1 (SOBIR1) to initiate downstream signaling (Liebrand et al., 2013; Albert et al., 2015). Although SOBIR1 has been shown to associate with INR in *Nicotiana benthamiana*, it is not yet known if SOBIR1 is necessary for immune signaling by PvINR (Steinbrenner et al., 2020). To determine whether PvINR requires SOBIR1

and whether the *p2xLYS1::LUZ* reflects downstream immune signaling pathways, we conducted reporter assays in *N. benthamiana sobir1* knockout plants, which previously showed compromised function of the tomato LRR-RLP Cf4 (Huang et al., 2021). Induction of luminescence by In11 treatment is absent in *sobir1* mutant plants and restored when either *A. thaliana SOBIR1* or *P. vulgaris SOBIR1* are coexpressed with *PvINR*. (Fig. 5). Thus, reporter activation is subject to similar requirements for LRR-RLP function as well-characterized PTI responses. This suggests that the *p2xLYS1::LUZ* construct serves as a useful tool not only for studying receptor-elicitor interactions but also downstream interactions important for immune activation and signaling.

Discussion

We describe here a genetically encoded reporter responsive to heterologously expressed PRRs in *N. benthamiana.* The *p2xLYS1::LUZ* reporter demonstrates robust PAMP sensitivity and does not require addition of exogenous enzyme substrate. Therefore, this reporter assay may be a useful tool for assessing immune activation by a number of diverse PRRs, including both receptor-like kinases and receptor-like proteins.

To develop this reporter, we first characterized the transcriptional modifications that occur in response to both *Agrobacterium* and elicitor perception by a heterologously expressed LRR-RLP. LRR-RLPs warrant further structural and functional

353 characterization, as they constitute a key class of PRRs involved in activating plant
354 innate immune responses (Jamieson et al., 2018; Albert et al., 2020; Steinbrenner,
355 2020). LRR-RLPs also include the first known receptor-ligand pair involved in defense
356 against a chewing herbivore (Steinbrenner et al., 2020). However, the specific
357 molecular interactions required for immune signaling by LRR-RLPs in plants remain
358 only partially understood, in part because no solved crystal structures of LRR-RLPs
359 have been reported. Although characterized LRR-RLPs require SUPPRESSOR OF
360 BIR1-1 (SOBIR1) and SOMATIC EMBRYOGENESIS RECEPTOR KINASEs (SERKs)
361 to activate immune signaling, the mechanisms underlying ligand binding and coreceptor
362 association are unclear (van der Burgh et al., 2019). As a result, we tailored our reporter
363 system toward heterologously expressed LRR-RLPs to aid in gathering deeper insights
364 into this important and incompletely understood group of plant cell surface immune
365 receptors. However, we also observed induction of luminescence in response to the
366 bacterial elicitor elf18 in tissue expressing *A. thaliana* EFR, a receptor-like kinase (RLK)
367 (Zipfel et al., 2006). As a result, this reporter could be useful for studying RLK signaling.
368 Additionally, recent studies describing the overlap between PTI and ETI signaling
369 suggest common signaling components (Ngou et al., 2021; Pruitt et al., 2021). As a
370 result, there is a possibility this reporter could serve to study intracellular immune
371 receptors and may be particularly useful when these receptors do not produce
372 hypersensitive responses.

373 Unsurprisingly, our transcriptomic analysis revealed that *Agrobacterium* treatment alone
374 resulted in large changes in gene expression. This demonstrates that *Agrobacterium*
375 strongly induces innate immunity in *N. benthamiana*, likely through recognition of

Agrobacterium PAMPs, resulting in large-scale transcriptional changes. Therefore, it is important to consider the role of *Agrobacterium* PAMPs in activating immunity. Interestingly, many genes that showed upregulation in response to In11 treatment were genes that were downregulated by *Agrobacterium* (Fig S1B-C). While likely due to timescales of *Agrobacterium* inoculation (24 hpi) versus In11 treatment (6 hpi), it is also possible that perception of Agrobacterium PAMPs by *N. benthamiana* is antagonized by simultaneous activation of immunity by the herbivore-associated In11 elicitor, a potential result of signaling conflict between SA and JA signaling (Li et al., 2019). *Agrobacterium* may activate biotroph-related immunity, whereas INR may activate necrotroph-related immunity through pathways downstream of SOBIR1. Because of the complex nature of these factors, we selected genes that showed upregulation in response to *Agrobacterium* that was further amplified by In11 treatment to identify a generic marker of immune activation by specific elicitor receptor interactions.

Although we identified four marker candidates, only one showed induction of luminescence in response to elicitor treatment (Fig. 3). We were either unable to clone the respective promoter region (*Niben101Scf04592g00020*, *Niben101Scf04652g00027*) or observed no luminescence in response to In11 treatment compared to water treatment (*Niben101Scf08566g08014*) (Supplementary Fig. S2). Although protocols exist to amplify difficult templates such as AT or GC-rich sequences (Dhatterwal et al., 2017; Sahdev et al., 2007), the complex nature of the *N. benthamiana* genome poses technical challenges in amplifying already evasive promoter regions (Bombarely et al., 2012). Furthermore, it is possible that promoter terminator incompatibility occurred between candidate promoter regions resulting in silencing of *LUZ* (P.-H. Wang et al.,

2020). Finally, it is possible that we failed to include the necessary cis-regulatory elements of the promoter region, as we decided on a somewhat arbitrary cutoff of 1.5 kb preceding the start codon of the gene. Trans-regulatory elements may also be necessary to mediate observed changes in gene expression in response to In11 treatment. As a result, improved understanding of plant transcriptional regulatory elements will facilitate efforts to identify and utilize additional highly responsive promoters under a variety of biotic stress conditions as tools to study plant immune responses.

The *pFBP_promoter_acceptor* construct is now publicly available to screen other candidate promoters through simple MoClo ligation of a promoter of interest. However, several considerations should be taken regarding the use of the FBP reporter. Unlike firefly luciferase, which is known to have a short half-life in the presence of luciferin (Van Leeuwen et al., 2000), it is suggested that the stability of fungal luciferase is more suitable for measuring changes over hours, limiting its utility on finer time scales (Khakhar et al., 2020). Induction of luminescence should as a result be viewed as a cumulative representation of reporter activity, rather than instantaneous measure of gene expression. Furthermore, production of fungal luciferin depends on availability of caffeic acid, causing luciferin availability to not be completely uniform across all plant tissues, and sustained periods of fungal luciferase activity to possibly deplete luciferin stores. Although these limitations remain largely negligible for the purpose of assessing specific receptor-elicitor interactions, they should be considered in situations where temporal and spatial aspects are of importance.

421 This system represents a potentially high-throughput and sensitive reporter for
422 assessing immune activation by heterologously expressed PRRs in *N. benthamiana*.
423 Although other systems retain power by being more sensitive to subtle immune
424 phenotypes and usefulness in characterizing endogenous immune signaling processes
425 in non-model organisms, the sensitivity, robustness, and ease of the FBP reporter
426 system make it useful for understanding cell surface receptor function in *N.*
427 *benthamiana*. As a result, this reporter represents a potentially valuable addition to the
428 plant immune biology toolkit, especially for large scale studies aimed at illuminating the
429 structure and function of cell surface immune receptors from diverse species.

430 **Acknowledgements**

431 We thank members of the Steinbrenner, Imaizumi and Nemhauser labs at UW Biology
432 for helpful discussion and comments. This work was supported by NSF grant IOS-
433 2139986 and the UW Mary Gates Endowment for Students.

434

435 **Author Contributions**

436 A.D.S. conducted the transcriptomic analysis. A.G.K.G. conducted subsequent
437 experiments. A.D.S. and A.G.K.G wrote the manuscript.

Materials Availability

Transcriptomic data are available in NCBI SRA (BioProject number pending). The *pFBP_promoter_acceptor* and *pFBP_2xNbLYS1::LUZ* constructs are available at Addgene (confirmation pending).

References

Adachi, H., Contreras, M. P., Harant, A., Wu, C., Derevnina, L., Sakai, T., Duggan, C., Moratto, E., Bozkurt, T. O., Maqbool, A., Win, J., & Kamoun, S. (2019). An N-terminal motif in NLR immune receptors is functionally conserved across distantly related plant species. *ELife*, *8*, e49956. https://doi.org/10.7554/eLife.49956

Albert, I., Böhm, H., Albert, M., Feiler, C. E., Imkampe, J., Wallmeroth, N., Brancato, C., Raaymakers, T. M., Oome, S., Zhang, H., Krol, E., Grefen, C., Gust, A. A., Chai, J., Hedrich, R., Van den Ackerveken, G., & Nürnberger, T. (2015). An RLP23–SOBIR1–BAK1 complex mediates NLP-triggered immunity. *Nature Plants*, *1*(10), 1–9. https://doi.org/10.1038/nplants.2015.140

Albert, I., Hua, C., Nürnberger, T., Pruitt, R. N., & Zhang, L. (2020). Surface Sensor Systems in Plant Immunity. *Plant Physiology*, *182*(4), 1582–1596. https://doi.org/10.1104/pp.19.01299

Aldon, D., Mbengue, M., Mazars, C., & Galaud, J.-P. (2018). Calcium Signalling in Plant Biotic Interactions. *International Journal of Molecular Sciences*, *19*(3), 665. https://doi.org/10.3390/ijms19030665

Anders, S., Pyl, P. T., & Huber, W. (2015). HTSeq—A Python framework to work with high-throughput sequencing data. *Bioinformatics*, *31*(2), 166–169.

https://doi.org/10.1093/bioinformatics/btu638

Berens, M. L., Berry, H. M., Mine, A., Argueso, C. T., & Tsuda, K. (2017). Evolution of Hormone Signaling Networks in Plant Defense. *Annual Review of Phytopathology*, *55*(1), 401–425. https://doi.org/10.1146/annurev-phyto-080516-035544

Bombarely, A., Rosli, H. G., Vrebalov, J., Moffett, P., Mueller, L. A., & Martin, G. B. (2012). A Draft Genome Sequence of Nicotiana benthamiana to Enhance Molecular Plant-Microbe Biology Research. *Molecular Plant-Microbe Interactions*, *25*(12), 1523–1530. https://doi.org/10.1094/MPMI-06-12-0148-TA

Boutrot, F., & Zipfel, C. (2017). Function, Discovery, and Exploitation of Plant Pattern Recognition Receptors for Broad-Spectrum Disease Resistance. *Annual Review of Phytopathology*, *55*, 257–286. https://doi.org/10.1146/annurev-phyto-080614-120106

Broekgaarden, C., Caarls, L., Vos, I. A., Pieterse, C. M. J., & Van Wees, S. C. M. (2015). Ethylene: Traffic Controller on Hormonal Crossroads to Defense. *Plant Physiology*, *169*(4), 2371–2379. https://doi.org/10.1104/pp.15.01020

Buscaill, P., Sanguankiattichai, N., Lee, Y. J., Kourelis, J., Preston, G., & van der Hoorn, R. A. L. (2021). Agromonas: A rapid disease assay for Pseudomonas syringae growth in agroinfiltrated leaves. *The Plant Journal*, *105*(3), 831–840. https://doi.org/10.1111/tpj.15056

de Jonge, R., Peter van Esse, H., Maruthachalam, K., Bolton, M. D., Santhanam, P., Saber, M. K., Zhang, Z., Usami, T., Lievens, B., Subbarao, K. V., & Thomma, B. P. H. J. (2012). Tomato immune receptor Ve1 recognizes effector of multiple

485 fungal pathogens uncovered by genome and RNA sequencing. *Proceedings of*
486 *the National Academy of Sciences*, *109*(13), 5110–5115.
487 https://doi.org/10.1073/pnas.1119623109
488 DeBlasio, S. L., Sylvester, A. W., & Jackson, D. (2010). Illuminating plant biology: Using
489 fluorescent proteins for high-throughput analysis of protein localization and
490 function in plants. *Briefings in Functional Genomics*, *9*(2), 129–138.
491 https://doi.org/10.1093/bfgp/elp060
492 DeFalco, T. A., Toyota, M., Phan, V., Karia, P., Moeder, W., Gilroy, S., & Yoshioka, K.
493 (2017). Using GCaMP3 to Study Ca2+ Signaling in Nicotiana Species. *Plant and*
494 *Cell Physiology*, *58*(7), 1173–1184. https://doi.org/10.1093/pcp/pcx053
495 Denoux, C., Galletti, R., Mammarella, N., Gopalan, S., Werck, D., De Lorenzo, G.,
496 Ferrari, S., Ausubel, F. M., & Dewdney, J. (2008). Activation of Defense
497 Response Pathways by OGs and Flg22 Elicitors in Arabidopsis Seedlings.
498 *Molecular Plant*, *1*(3), 423–445. https://doi.org/10.1093/mp/ssn019
499 Dhatterwal, P., Mehrotra, S., & Mehrotra, R. (2017). Optimization of PCR conditions for
500 amplifying an AT-rich amino acid transporter promoter sequence with high
501 number of tandem repeats from Arabidopsis thaliana. *BMC Research Notes*, *10*,
502 638. https://doi.org/10.1186/s13104-017-2982-1
503 Earley, K. W., Haag, J. R., Pontes, O., Opper, K., Juehne, T., Song, K., & Pikaard, C. S.
504 (2006). Gateway-compatible vectors for plant functional genomics and
505 proteomics. *The Plant Journal*, *45*(4), 616–629. https://doi.org/10.1111/j.1365-
506 313X.2005.02617.x
507 Engler, C., Youles, M., Gruetzner, R., Ehnert, T.-M., Werner, S., Jones, J. D. G., Patron,

508 N. J., & Marillonnet, S. (2014). A Golden Gate Modular Cloning Toolbox for
509 Plants. *ACS Synthetic Biology*, *3*(11), 839–843.
510 https://doi.org/10.1021/sb4001504
511 Furuhata, Y., Sakai, A., Murakami, T., Nagasaki, A., & Kato, Y. (2020). Bioluminescent
512 imaging of Arabidopsis thaliana using an enhanced Nano-lantern luminescence
513 reporter system. *PLoS ONE*, *15*(1), e0227477.
514 https://doi.org/10.1371/journal.pone.0227477
515 Goodin, M. M., Zaitlin, D., Naidu, R. A., & Lommel, S. A. (2008). Nicotiana
516 benthamiana: Its History and Future as a Model for Plant–Pathogen Interactions.
517 *Molecular Plant-Microbe Interactions*, *21*(8), 1015–1026.
518 https://doi.org/10.1094/MPMI-21-8-1015
519 Haugwitz, M., Nourzaie, O., Garachtchenko, T., Hu, L., Gandlur, S., Olsen, C., Farmer,
520 A., Chaga, G., & Sagawa, H. (2008). Multiplexing Bioluminescent and
521 Fluorescent Reporters to Monitor Live Cells. *Current Chemical Genomics*, *1*, 11–
522 19. https://doi.org/10.2174/1875397300801010011
523 He, Y., Zhang, T., Sun, H., Zhan, H., & Zhao, Y. (2020). A reporter for noninvasively
524 monitoring gene expression and plant transformation. *Horticulture Research*,
525 *7*(1), 1–6. https://doi.org/10.1038/s41438-020-00390-1
526 Huang, W. R. H., Schol, C., Villanueva, S. L., Heidstra, R., & Joosten, M. H. A. J.
527 (2021). Knocking out SOBIR1 in Nicotiana benthamiana abolishes functionality of
528 transgenic receptor-like protein Cf-4. *Plant Physiology*, *185*(2), 290–294.
529 https://doi.org/10.1093/plphys/kiaa047
530 Jamieson, P. A., Shan, L., & He, P. (2018). Plant cell surface molecular cypher:

Receptor-like proteins and their roles in immunity and development. *Plant Science*, *274*, 242–251. https://doi.org/10.1016/j.plantsci.2018.05.030

Jutras, P. V., Soldan, R., Dodds, I., Schuster, M., Preston, G. M., & van der Hoorn, R. A. L. (2021). AgroLux: Bioluminescent Agrobacterium to improve molecular pharming and study plant immunity. *The Plant Journal*, *108*(2), 600–612. https://doi.org/10.1111/tpj.15454

Katoh, K., Rozewicki, J., & Yamada, K. D. (2019). MAFFT online service: Multiple sequence alignment, interactive sequence choice and visualization. *Briefings in Bioinformatics*, *20*(4), 1160–1166. https://doi.org/10.1093/bib/bbx108

Kay, R., Chan, A., Daly, M., & McPherson, J. (1987). Duplication of CaMV 35S Promoter Sequences Creates a Strong Enhancer for Plant Genes. *Science*, *236*(4806), 1299–1302.

Khakhar, A., Starker, C. G., Chamness, J. C., Lee, N., Stokke, S., Wang, C., Swanson, R., Rizvi, F., Imaizumi, T., & Voytas, D. F. (2020). Building customizable auto-luminescent luciferase-based reporters in plants. *ELife*, *9*, e52786. https://doi.org/10.7554/eLife.52786

Kim, D., Paggi, J. M., Park, C., Bennett, C., & Salzberg, S. L. (2019). Graph-based genome alignment and genotyping with HISAT2 and HISAT-genotype. *Nature Biotechnology 37(8),* 907–915. https://doi.org/10.1038/s41587-019-0201-4

Kuraku, S., Zmasek, C. M., Nishimura, O., & Katoh, K. (2013). ALeaves facilitates on-demand exploration of metazoan gene family trees on MAFFT sequence alignment server with enhanced interactivity. *Nucleic Acids Research*, *41*(W1), W22–W28. https://doi.org/10.1093/nar/gkt389

554 Li, N., Han, X., Feng, D., Yuan, D., & Huang, L.-J. (2019). Signaling Crosstalk between
555 Salicylic Acid and Ethylene/Jasmonate in Plant Defense: Do We Understand
556 What They Are Whispering? *International Journal of Molecular Sciences*, *20*(3),
557 671. https://doi.org/10.3390/ijms20030671
558 Liebrand, T. W. H., van den Berg, G. C. M., Zhang, Z., Smit, P., Cordewener, J. H. G.,
559 America, A. H. P., Sklenar, J., Jones, A. M. E., Tameling, W. I. L., Robatzek, S.,
560 Thomma, B. P. H. J., & Joosten, M. H. A. J. (2013). Receptor-like kinase
561 SOBIR1/EVR interacts with receptor-like proteins in plant immunity against
562 fungal infection. *Proceedings of the National Academy of Sciences*, *110*(24),
563 10010–10015. https://doi.org/10.1073/pnas.1220015110
564 Liu, D., Shi, L., Han, C., Yu, J., Li, D., & Zhang, Y. (2012). Validation of Reference
565 Genes for Gene Expression Studies in Virus-Infected Nicotiana benthamiana
566 Using Quantitative Real-Time PCR. *PLoS ONE*, *7*(9), e46451.
567 https://doi.org/10.1371/journal.pone.0046451
568 Liu, X., Grabherr, H. M., Willmann, R., Kolb, D., Brunner, F., Bertsche, U., Kühner, D.,
569 Franz-Wachtel, M., Amin, B., Felix, G., Ongena, M., Nürnberger, T., & Gust, A. A.
570 (2014). Host-induced bacterial cell wall decomposition mediates pattern-triggered
571 immunity in Arabidopsis. *ELife*, *3*, e01990. https://doi.org/10.7554/eLife.01990
572 Love, M. I., Huber, W., & Anders, S. (2014). Moderated estimation of fold change and
573 dispersion for RNA-seq data with DESeq2. *Genome Biology*, *15*(12), 550.
574 https://doi.org/10.1186/s13059-014-0550-8
575 Melotto, M., Zhang, L., Oblessuc, P. R., & He, S. Y. (2017). Stomatal Defense a Decade
576 Later. *Plant Physiology*, *174*(2), 561–571. https://doi.org/10.1104/pp.16.01853

577 Miller, M. A., Pfeiffer, W., & Schwartz, T. (2010). Creating the CIPRES Science
578 Gateway for inference of large phylogenetic trees. *Proceedings of the Gateway*
579 *Computing Environments Workshop (GCE)*, 1–8.
580 https://doi.org/10.1109/GCE.2010.5676129
581 Mitiouchkina, T., Mishin, A. S., Somermeyer, L. G., Markina, N. M., Chepurnyh, T. V.,
582 Guglya, E. B., Karataeva, T. A., Palkina, K. A., Shakhova, E. S., Fakhranurova,
583 L. I., Chekova, S. V., Tsarkova, A. S., Golubev, Y. V., Negrebetsky, V. V.,
584 Dolgushin, S. A., Shalaev, P. V., Shlykov, D., Melnik, O. A., Shipunova, V. O., …
585 Sarkisyan, K. S. (2020). Plants with genetically encoded autoluminescence.
586 *Nature Biotechnology*, *38*(8), 944–946. https://doi.org/10.1038/s41587-020-0500-
587 9
588 Mott, G. A., Desveaux, D., & Guttman, D. S. (2018). A High-Sensitivity, Microtiter-Based
589 Plate Assay for Plant Pattern-Triggered Immunity. *Molecular Plant-Microbe*
590 *Interactions*, *31*(5), 499–504. https://doi.org/10.1094/MPMI-11-17-0279-TA
591 Navarro, L., Zipfel, C., Rowland, O., Keller, I., Robatzek, S., Boller, T., & Jones, J. D. G.
592 (2004). The transcriptional innate immune response to flg22. Interplay and
593 overlap with Avr gene-dependent defense responses and bacterial pathogenesis.
594 *Plant Physiology*, *135*(2), 1113–1128. https://doi.org/10.1104/pp.103.036749
595 Ngou, B. P. M., Ahn, H.-K., Ding, P., & Jones, J. D. G. (2021). Mutual potentiation of
596 plant immunity by cell-surface and intracellular receptors. *Nature*, *592*(7852),
597 110–115. https://doi.org/10.1038/s41586-021-03315-7
598 Nguyen, H. P., Chakravarthy, S., Velásquez, A. C., McLane, H. L., Zeng, L.,
599 Nakayashiki, H., Park, D.-H., Collmer, A., & Martin, G. B. (2010). Methods to

study PAMP-triggered immunity using tomato and Nicotiana benthamiana. *Molecular Plant-Microbe Interactions*, *23*(8), 991–999. https://doi.org/10.1094/MPMI-23-8-0991

Pruitt, R. N., Locci, F., Wanke, F., Zhang, L., Saile, S. C., Joe, A., Karelina, D., Hua, C., Fröhlich, K., Wan, W.-L., Hu, M., Rao, S., Stolze, S. C., Harzen, A., Gust, A. A., Harter, K., Joosten, M. H. A. J., Thomma, B. P. H. J., Zhou, J.-M., … Nürnberger, T. (2021). The EDS1–PAD4–ADR1 node mediates Arabidopsis pattern-triggered immunity. *Nature*, *598*(7881), 495–499. https://doi.org/10.1038/s41586-021-03829-0

Qi, J., Wang, J., Gong, Z., & Zhou, J.-M. (2017). Apoplastic ROS signaling in plant immunity. *Current Opinion in Plant Biology*, *38*, 92–100. https://doi.org/10.1016/j.pbi.2017.04.022

Sahdev, S., Saini, S., Tiwari, P., Saxena, S., & Singh Saini, K. (2007). Amplification of GC-rich genes by following a combination strategy of primer design, enhancers and modified PCR cycle conditions. *Molecular and Cellular Probes*, *21*(4), 303–307. https://doi.org/10.1016/j.mcp.2007.03.004

Schmelz, E. A., Carroll, M. J., LeClere, S., Phipps, S. M., Meredith, J., Chourey, P. S., Alborn, H. T., & Teal, P. E. A. (2006). Fragments of ATP synthase mediate plant perception of insect attack. *Proceedings of the National Academy of Sciences*, *103*(23), 8894–8899. https://doi.org/10.1073/pnas.0602328103

Segretin, M. E., Pais, M., Franceschetti, M., Chaparro-Garcia, A., Bos, J. I. B., Banfield, M. J., & Kamoun, S. (2014). Single Amino Acid Mutations in the Potato Immune Receptor R3a Expand Response to Phytophthora Effectors. *Molecular Plant-*

Microbe Interactions, *27*(7), 624–637. https://doi.org/10.1094/MPMI-02-14-0040-R

Stamatakis, A. (2014). RAxML version 8: A tool for phylogenetic analysis and post-analysis of large phylogenies. *Bioinformatics*, *30*(9), 1312–1313. https://doi.org/10.1093/bioinformatics/btu033

Steinbrenner, A. D. (2020). The evolving landscape of cell surface pattern recognition across plant immune networks. *Current Opinion in Plant Biology*, *56*, 135–146. https://doi.org/10.1016/j.pbi.2020.05.001

Steinbrenner, A. D., Goritschnig, S., & Staskawicz, B. J. (2015). Recognition and Activation Domains Contribute to Allele-Specific Responses of an Arabidopsis NLR Receptor to an Oomycete Effector Protein. *PLOS Pathogens*, *11*(2), e1004665. https://doi.org/10.1371/journal.ppat.1004665

Steinbrenner, A. D., Muñoz-Amatriaín, M., Chaparro, A. F., Aguilar-Venegas, J. M., Lo, S., Okuda, S., Glauser, G., Dongiovanni, J., Shi, D., Hall, M., Crubaugh, D., Holton, N., Zipfel, C., Abagyan, R., Turlings, T. C. J., Close, T. J., Huffaker, A., & Schmelz, E. A. (2020). A receptor-like protein mediates plant immune responses to herbivore-associated molecular patterns. *Proceedings of the National Academy of Sciences*, *117*(49), 31510–31518. https://doi.org/10.1073/pnas.2018415117

Thorne, N., Inglese, J., & Auld, D. S. (2010). Illuminating insights into firefly luciferase and other bioluminescent reporters used in chemical biology. *Chemistry & Biology*, *17*(6), 646–657. https://doi.org/10.1016/j.chembiol.2010.05.012

Toyota, M., Spencer, D., Sawai-Toyota, S., Jiaqi, W., Zhang, T., Koo, A. J., Howe, G.

646 A., & Gilroy, S. (2018). Glutamate triggers long-distance, calcium-based plant
647 defense signaling. *Science*, *361*(6407), 1112–1115.
648 https://doi.org/10.1126/science.aat7744
649 van der Burgh, A. M., Postma, J., Robatzek, S., & Joosten, M. H. A. J. (2019). Kinase
650 activity of SOBIR1 and BAK1 is required for immune signalling. *Molecular Plant*
651 *Pathology*, *20*(3), 410–422. https://doi.org/10.1111/mpp.12767
652 Van Leeuwen, W., Hagendoorn, M. J. M., Ruttink, T., Van Poecke, R., Van Der Plas, L.
653 H. W., & Van Der Krol, A. R. (2000). The use of the luciferase reporter system for
654 in planta gene expression studies. *Plant Molecular Biology Reporter*, *18*(2), 143–
655 144. https://doi.org/10.1007/BF02824024
656 Wang, P.-H., Kumar, S., Zeng, J., McEwan, R., Wright, T. R., & Gupta, M. (2020).
657 Transcription Terminator-Mediated Enhancement in Transgene Expression in
658 Maize: Preponderance of the AUGAAU Motif Overlapping With Poly(A) Signals.
659 *Frontiers in Plant Science*, *11*.
660 https://www.frontiersin.org/article/10.3389/fpls.2020.570778
661 Wang, Y., Li, X., Fan, B., Zhu, C., & Chen, Z. (2021). Regulation and Function of
662 Defense-Related Callose Deposition in Plants. *International Journal of Molecular*
663 *Sciences*, *22*(5), 2393. https://doi.org/10.3390/ijms22052393
664 Zhang, L., Hua, C., Pruitt, R. N., Qin, S., Wang, L., Albert, I., Albert, M., van Kan, J. A.
665 L., & Nürnberger, T. (2021). Distinct immune sensor systems for fungal
666 endopolygalacturonases in closely related Brassicaceae. *Nature Plants*, *7*(9),
667 1254–1263. https://doi.org/10.1038/s41477-021-00982-2
668 Zhang, L., Kars, I., Essenstam, B., Liebrand, T. W. H., Wagemakers, L., Elberse, J.,

669 Tagkalaki, P., Tjoitang, D., Ackerveken, G. van den, & Kan, J. A. L. van. (2014).
670 Fungal Endopolygalacturonases Are Recognized as Microbe-Associated
671 Molecular Patterns by the Arabidopsis Receptor-Like Protein
672 RESPONSIVENESS TO BOTRYTIS POLYGALACTURONASES1. *Plant*
673 *Physiology*, *164*(1), 352–364. https://doi.org/10.1104/pp.113.230698
674 Zhang, Z., Fradin, E., de Jonge, R., van Esse, H. P., Smit, P., Liu, C.-M., & Thomma, B.
675 P. H. J. (2013). Optimized Agroinfiltration and Virus-Induced Gene Silencing to
676 Study Ve1-Mediated Verticillium Resistance in Tobacco. *Molecular Plant-Microbe*
677 *Interactions*, *26*(2), 182–190. https://doi.org/10.1094/MPMI-06-12-0161-R
678 Zipfel, C., Kunze, G., Chinchilla, D., Caniard, A., Jones, J. D. G., Boller, T., & Felix, G.
679 (2006). Perception of the bacterial PAMP EF-Tu by the receptor EFR restricts
680 Agrobacterium-mediated transformation. *Cell*, *125*(4), 749–760.
681 https://doi.org/10.1016/j.cell.2006.03.037

682 **Figure Legends**

683

684 **Figure 1. Agrobacterium and In11-induced changes in *N. benthamiana* gene**
685 **expression.** A, Venn diagram displaying number of significantly differentially expressed
686 genes (DEGs) upregulated by Agrobacterium relative to mock-treated tissue. B,
687 Agrobacterium-downregulated genes. Treatments are labeled as follows: AH,
688 Agrobacterium + H2O, AI, Agrobacterium + In11, H, Mock infiltrated leaf tissue. See Fig.
689 S1 for treatment details. Top ten genes in both categories with largest log2(fold-change)
690 (FC) are displayed at right. P-value indicates statistical significance with standard Wald
691 test. Adj. P indicates significance after correction for multiple comparisons (Benjamani-
692 Hochberg, BH). C, Candidate genes induced by In11 in the presence of Agrobacterium.
693 While only one DEG was observed after BH correction, 9 genes were induced by In11
694 uncorrected for multiple comparisons (Fig. S1).
695

696 **Figure 2. RT-qPCR validation of candidate marker genes.** Boxplots indicate the
697 mean log_2(fold change) between water and In11 treated tissue (log_2(FC) In11 vs H_2O) of
698 gene expression from *N. benthamiana* plants expressing either p*35s::PvINR* or an

699 empty vector (EV) over four biological replicates. Student's t-tests were conducted to
700 determine significance (n.s.: not significant p>.05, *: p<0.05, **: p<0.01, ***: p<0.001).
701
702 **Figure 3. A *Nicotiana benthamiana LYS1* homolog serves as a marker of inceptin**
703 **response.** A, Leaves were coinfiltrated with *p35s::PvINR* and *pLYS1::LUZ* across the
704 proximal portion of the leaf, and *p35s::PvINR* and *p2xLYS1::LUZ* across the distal
705 portion of the leaf. 48 hours after infiltration, one half of the leaf was infiltrated with
706 sterile water, and the other half was infiltrated with 1 μM In11. Images were obtained 6
707 hours after peptide treatment, and ASI was quantified in ImageJ. Left, boxplots show
708 the average ASI of three independent biological replicates. Letters represent
709 significantly different means (One-way ANOVA and post-hoc Tukey's HSD tests, p<.05).
710 Right, a representative leaf image of one biological replicate is depicted. B, Leaves
711 were co-infiltrated with *p35s::PvINR* and *p2xLYS1::LUZ* in six distinct regions of the
712 leaf. 48 hours after infiltration each zone was infiltrated with sterile water or a series of
713 In11 concentrations. Imaging and quantification were conducted as in A.
714
715 **Figure 4. The *p2xLYS1::LUZ* construct acts as a generic reporter for plant pattern**
716 **recognition receptors.** Leaves of *N. benthamiana* plants were coinfiltrated with the
717 *p2xLYS1::LUZ* reporter construct and either A) empty vector, B) *35s::PvINR,* C)
718 *35s::AtEFR,* or D) *35s::AtRLP23* in four distinct regions. 48 hours after infiltration, each
719 region was infiltrated with either sterile water, 1 μM In11, 1 μM elf18, or 1 μM nlp20
720 peptide. Images were obtained 6 hours after peptide treatment, and ASI was quantified
721 in ImageJ. Left, boxplots show the average ASI of six independent biological replicates.
722 Letters represent significantly different means (One-way ANOVA and post-hoc Tukey's
723 HSD tests, p<.05). Right, a representative leaf image of one biological replicate is
724 depicted.
725
726 **Figure 5. SOBIR1 is necessary for activation of luminescence by PvINR.** Leaves of
727 *Nicotiana benthamiana sobir1* knockout plants were coinfiltrated with the
728 *pFBP_2xLYS1::LUZ* reporter construct, *p35s::PvINR* and either: empty vector (EV); A)
729 *p35s::PvSOBIR1; or B) p35s::AtSOBIR1* , repeated for three biological replicates. 48
730 hours after infiltration, each region of interest was infiltrated with either sterile water or 1
731 μM In11. Images were obtained 6 hours after peptide treatment, and ASI was quantified
732 in ImageJ. Left, boxplots show the average ASI of three independent biological
733 replicates. Letters represent significantly different means (One-way ANOVA and post-
734 hoc Tukey's HSD tests, p<.05). Right, a representative leaf image of one biological
735 replicate is depicted.

A

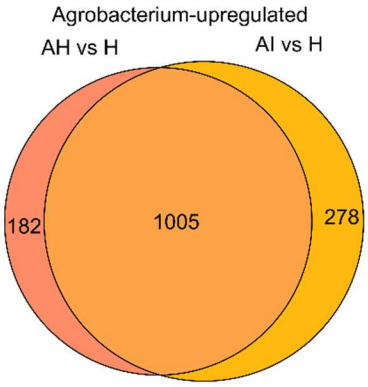

Gene	Niben101 Functional Annotation	Agro + H2O (AH) vs H2O (H)		
		log2(FC)	p-value	adj. p
Niben101Scf09186g00006	trypsin proteinase inhibitor precursor [Nicotiana tabacum]	-3.43	9.35E-20	4.39E-17
Niben101Scf01685g12005	Xyloglucan endotransglucosylase/hydrolase protein 9	-2.94	1.44E-14	3.69E-12
Niben101Scf05216g09026	PDZ, K-box, TPR	-1.85	4.07E-14	9.95E-12
Niben101Scf00887g02006	Ornithine decarboxylase	-4.92	1.21E-13	2.80E-11
Niben101Scf11490g00008	Thiamine thiazole synthase	-1.40	9.52E-13	1.86E-10
Niben101Scf07638g01010	Seed storage 2S albumin superfamily protein	-3.06	1.99E-12	3.53E-10
Niben101Scf03404g00007	BnaA06g36820D [Brassica napus]	-2.33	2.74E-12	4.73E-10
Niben101Scf05073g02002	Transcription factor EB	-4.93	3.93E-11	5.43E-09
Niben101Scf10316g01005	carbohydrate binding protein, putative [Ricinus communis]	-2.66	7.62E-11	1.01E-08
Niben101Scf05782g00010	Oxygen-evolving enhancer protein 2-1, chloroplastic	-1.68	9.77E-11	1.25E-08

B

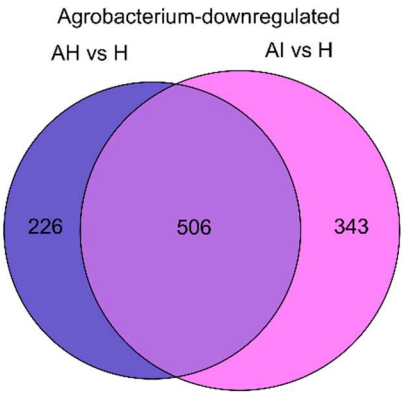

Gene	Niben101 Functional Annotation	Agro + H2O (AH) vs H2O (H)		
		log2(FC)	p-value	adj. p
Niben101Scf01084g03003	No annotation (BLASTX: NbSAR8.2d)	7.82	5.14E-123	1.21E-118
Niben101Scf03385g02011	Plant basic secretory protein (BSP) protein	7.82	2.39E-110	2.80E-106
Niben101Scf35444g00004	Glutathione S-transferase U8	6.84	3.57E-85	2.79E-81
Niben101Scf02819g00005	Early nodulin-like protein 1	7.42	2.47E-69	1.45E-65
Niben101Scf02041g00002	Chitinase 8	4.66	7.48E-67	3.51E-63
Niben101Scf10735g00016	Major pollen allergen Bet v 1-M/N	5.17	9.52E-58	3.73E-54
Niben101Scf02410g00002	Chitinase 9	7.30	1.92E-47	6.43E-44
Niben101Scf05404g09001	Glutathione S-transferase U8	8.25	7.11E-44	2.09E-40
Niben101Scf02171g00007	chitinase [Zea mays subsp. parviglumis]	7.25	1.20E-42	3.14E-39
Niben101Scf02203g05002	3-hydroxy-3-methylglutaryl-coenzyme A reductase	5.10	2.00E-41	4.70E-38

C

Gene	Niben101 Functional Annotation	Agro + In11 (AI) vs Agro + H2O (AH)			Agro + H2O (AH) vs H2O (H)		
		log2(FC)	p-value	adj. p	log2(FC)	p-value	adj. p
Niben101Scf08566g08014	Peroxidase N1	2.05	2.97E-09	1.08E-04	2.85	1.45E-12	2.70E-10
Niben101Scf04592g00020	BURP domain-containing protein 3	2.40	1.00E-04	1.00E+00	5.16	9.53E-05	2.43E-03
Niben101Scf02513g05010	Peroxidase N1	1.36	4.79E-04	1.00E+00	4.74	1.99E-20	9.95E-18
Niben101Scf09387g01003	Seed storage 2S albumin superfamily protein	1.22	3.18E-03	1.00E+00	5.35	3.66E-15	1.02E-12
Niben101Scf03444g02004	BAG family molecular chaperone regulator 2	1.32	4.13E-03	1.00E+00	2.16	5.03E-04	9.11E-03
Niben101Scf02411g01001	Peroxidase 4	1.02	6.73E-03	1.00E+00	5.01	3.08E-08	2.36E-06
Niben101Scf06684g03003	Acidic endochitinase	2.13	2.21E-02	1.00E+00	3.29	2.73E-02	1.77E-01
Niben101Scf01534g02007	Annexin D4	1.02	4.42E-02	1.00E+00	1.69	2.38E-03	3.05E-02
Niben101Scf04652g00027	Unknown protein	1.53	4.80E-02	1.00E+00	2.64	3.71E-02	2.18E-01

Figure 1. Agrobacterium and In11-induced changes in *N. benthamiana* gene expression. A, Venn diagram displaying number of significantly differentially expressed genes (DEGs) upregulated by Agrobacterium relative to mock-treated tissue. B, Agrobacterium-downregulated genes. Treatments are labeled as follows: AH, Agrobacterium + H2O, AI, Agrobacterium + In11, H, Mock infiltrated leaf tissue. See Fig. S1 for treatment details. Top ten genes in both categories with largest log2(fold-change) (FC) are displayed at right. P-value indicates statistical significance with standard Wald test. Adj. P indicates significance after correction for multiple comparisons (Benjamini-Hochberg, BH). C, Candidate genes induced by In11 in the presence of Agrobacterium. While only one DEG was observed after BH correction, 9 genes were induced by In11 uncorrected for multiple comparisons (Fig. S1).

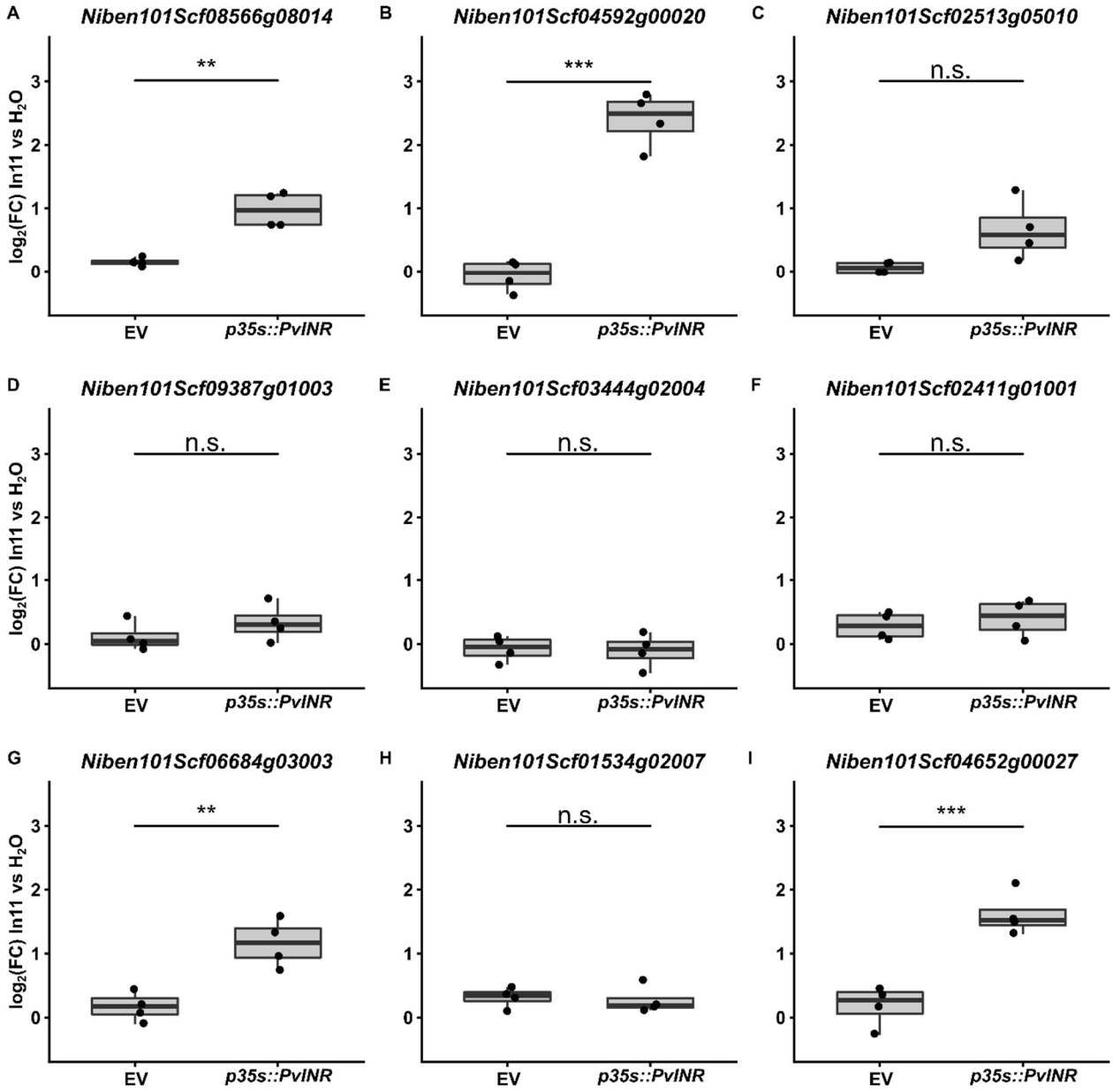

Figure 2. RT-qPCR validation of candidate marker genes.
Boxplots indicate the mean log_2(fold change) between water and In11 treated tissue (log_2(FC) In11 vs H_2O) of gene expression from *N. benthamiana* plants expressing either p*35s::PvINR* or an empty vector (EV) over four biological replicates. Student's t-tests were conducted to determine significance (n.s.: not significant p>.05, *: p<0.05, **: p<0.01, ***: p<0.001).

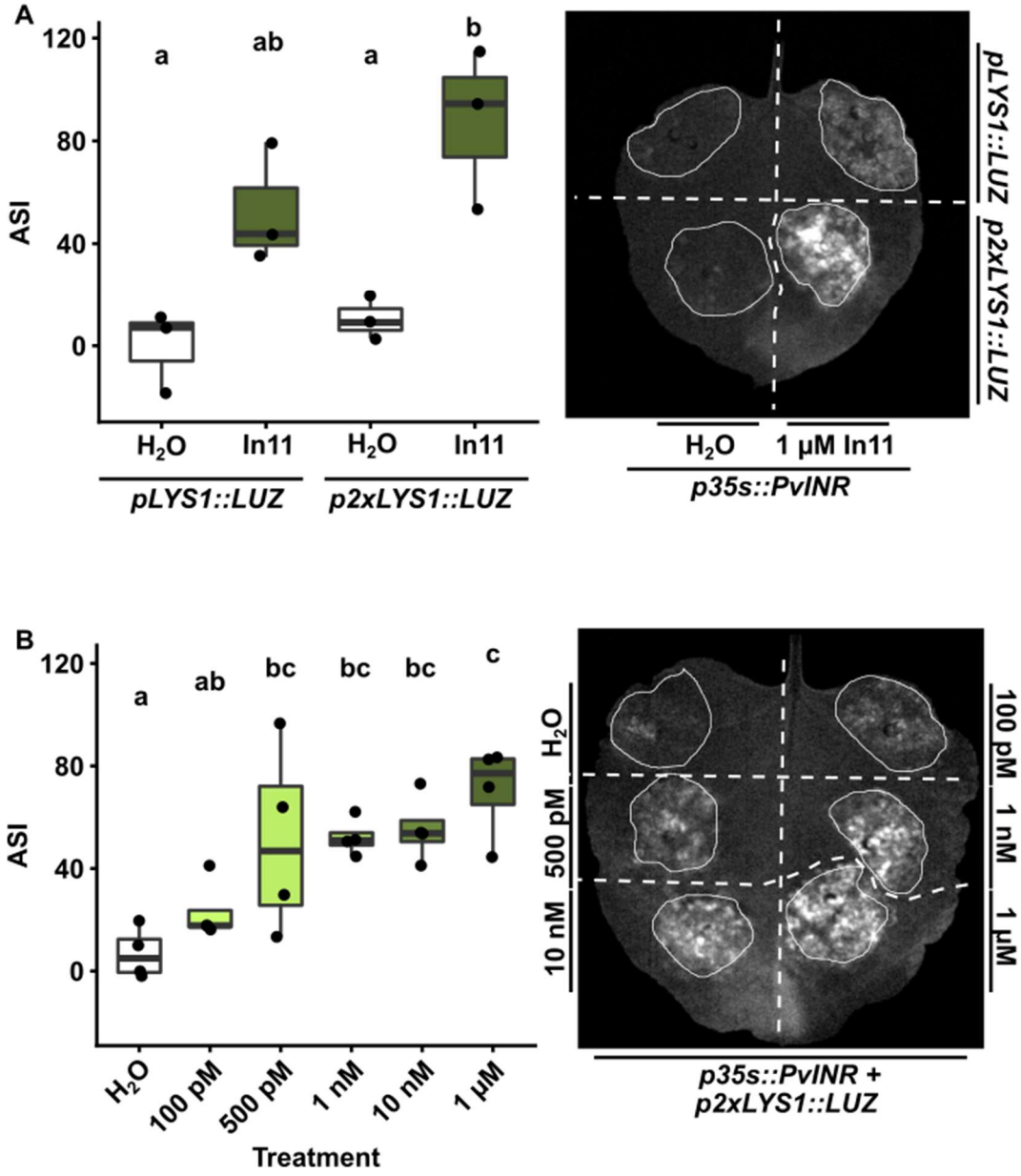

Figure 3. A *Nicotiana benthamiana LYS1* homolog serves as a marker of inceptin response. A, Leaves were coinfiltrated with *p35s::PvINR* and *pLYS1::LUZ* across the proximal portion of the leaf, and *p35s::PvINR* and *p2xLYS1::LUZ* across the distal portion of the leaf. 48 hours after infiltration, one half of the leaf was infiltrated with sterile water, and the other half was infiltrated with 1 µM In11. Images were obtained 6 hours after peptide treatment, and ASI was quantified in ImageJ. Left, boxplots show the average ASI of three independent biological replicates. Letters represent significantly different means (One-way ANOVA and post-hoc Tukey's HSD tests, $p<.05$). Right, a representative leaf image of one biological replicate is depicted. B, Leaves were co-infiltrated with *p35s::PvINR* and *p2xLYS1::LUZ* in six distinct regions of the leaf. 48 hours after infiltration each zone was infiltrated with sterile water or a series of In11 concentrations. Imaging and quantification were conducted as in A.

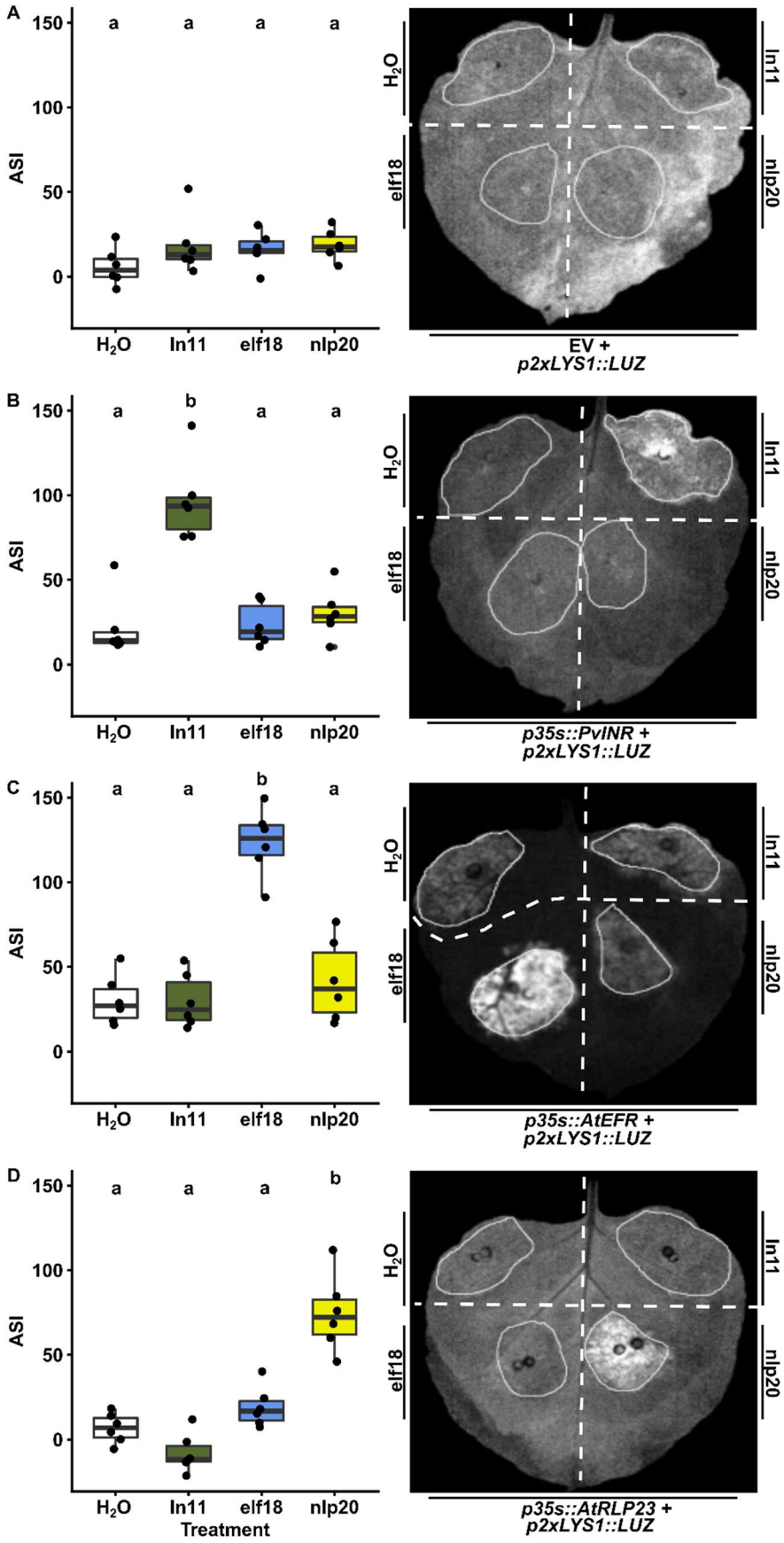

Figure 4. The *p2xLYS1::LUZ* construct acts as a generic reporter for plant pattern recognition receptors. Leaves of *N. benthamiana* plants were coinfiltrated with the *p2xLYS1::LUZ* reporter construct and either A) empty vector, B) *35s::PvINR,* C) *35s::AtEFR,* or D) *35s::AtRLP23* in four distinct regions. 48 hours after infiltration, each region was infiltrated with either sterile water, 1 µM In11, 1 µM elf18, or 1 µM nlp20 peptide. Images were obtained 6 hours after peptide treatment, and ASI was quantified in ImageJ. Left, boxplots show the average ASI of six independent biological replicates. Letters represent significantly different means (One-way ANOVA and post-hoc Tukey's HSD tests, p<.05). Right, a representative leaf image of one biological replicate is depicted.

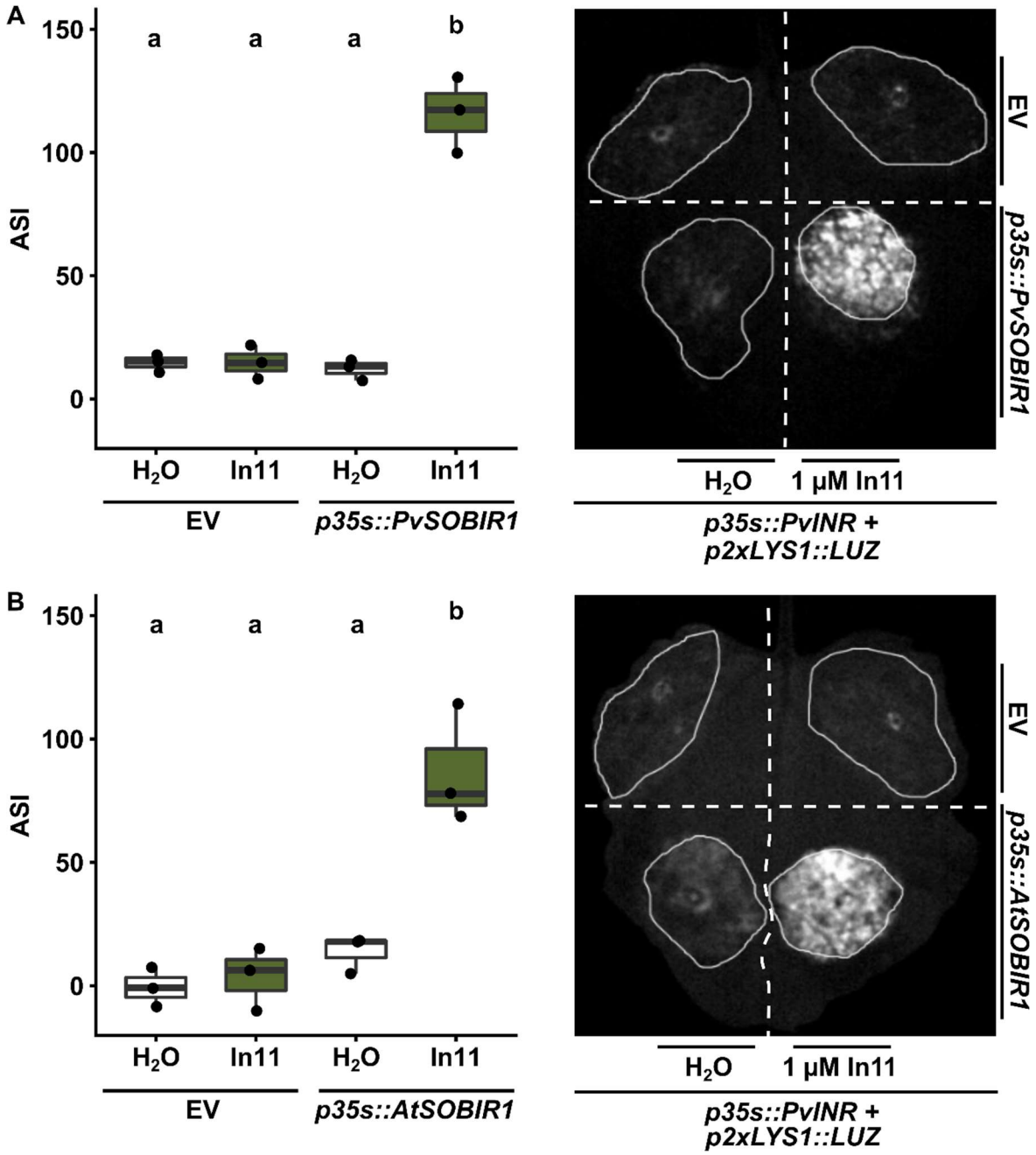

Figure 5. SOBIR1 is necessary for activation of luminescence by PvINR. Leaves of *Nicotiana benthamiana sobir1* knockout plants were coinfiltrated with the *pFBP_2xLYS1::LUZ* reporter construct, *p35s::PvINR* and either: empty vector (EV); A) *p35s::PvSOBIR1; or B) p35s::AtSOBIR1* , repeated for three biological replicates. 48 hours after infiltration, each region of interest was infiltrated with either sterile water or 1 µM In11. Images were obtained 6 hours after peptide treatment, and ASI was quantified in ImageJ. Left, boxplots show the average ASI of three independent biological replicates. Letters represent significantly different means (One-way ANOVA and post-hoc Tukey's HSD tests, $p<.05$). Right, a representative leaf image of one biological replicate is depicted.

Supplementary Figures

Pg 2. Supplementary Figure S1. Treatment details and transcriptional changes without correction for multiple comparisons.

Pg 3. Supplementary Figure S2. A modified FBP construct for rapid cloning and testing of putative promoter regions.

Pg 4. Supplemental Figure S3. The putative promoter region of *Niben101Scf08566g08014* does not serve as a marker of In11 response.

Pg 5. Supplemental Figure S4. The In11-upregulated gene *Niben101Scf06684g03003.1* is a homolog of *A. thaliana LYS1*.

Pg 6. Supplementary Figure S5. The *LYS1* Promoter Drives *LUZ* weaker than the strong constitutive *CaMV35s* promoter.

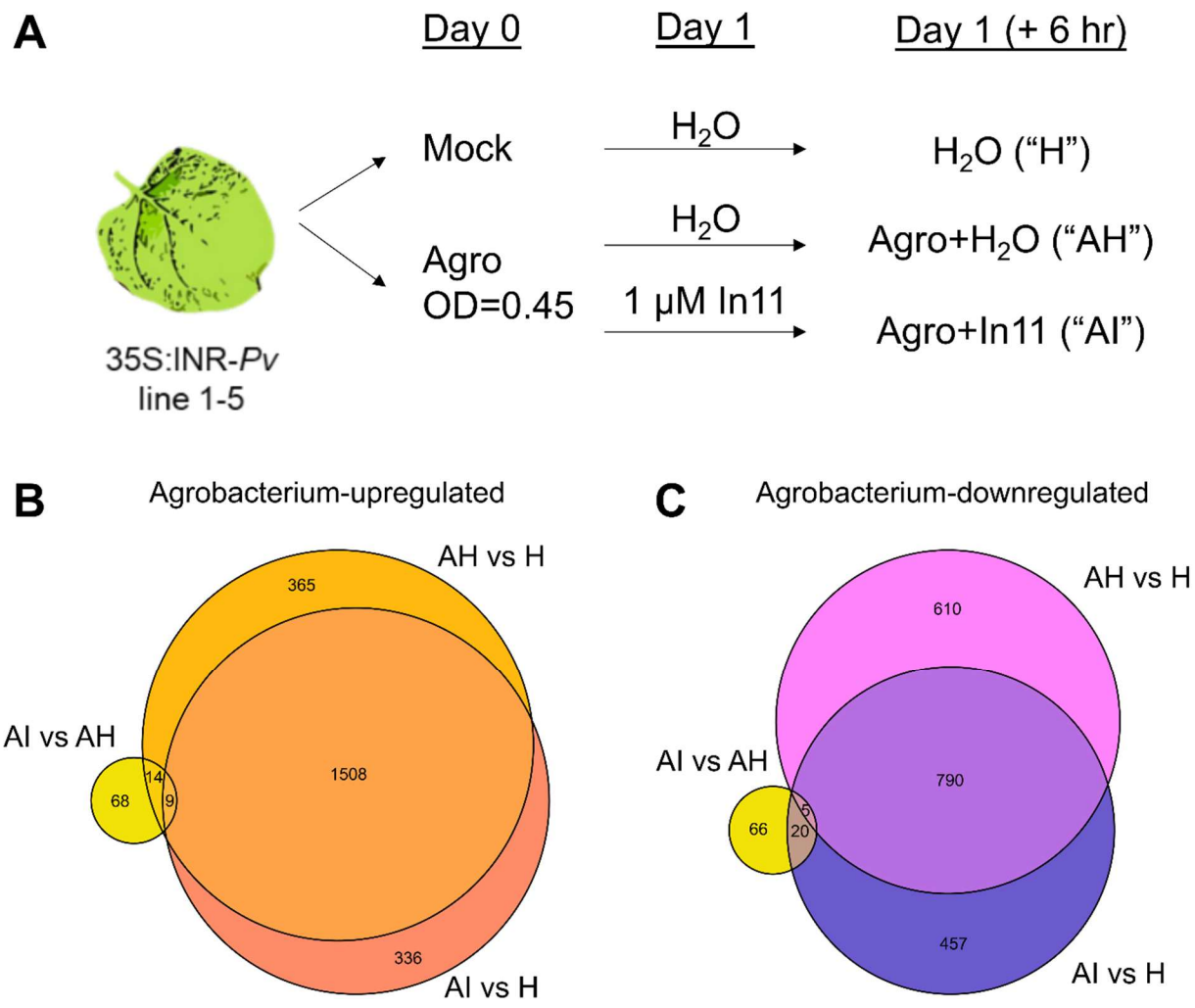

Supplementary Figure S1. Treatment details and transcriptional changes without correction for multiple comparisons.
A**,** *N. benthamiana* line 1-5 was infiltrated with water (mock) or Agrobacterium and then infiltrated at 24 hpi. Three treatments were collected for RNAseq analysis as indicated. Treatments are labeled as follows: AH, Agrobacterium + H2O, AI, Agrobacterium + In11, H, Mock infiltrated leaf tissue. B-C, Venn diagram displaying number of genes upregulated by In11 in the presence of Agrobacterium (AI vs AH, yellow), and genes B) upregulated by Agrobacterium or C) downregulated by Agrobacterium (Wald test, p-value < 0.05, no correction for multiple comparisons by Benjamini-Hochberg).

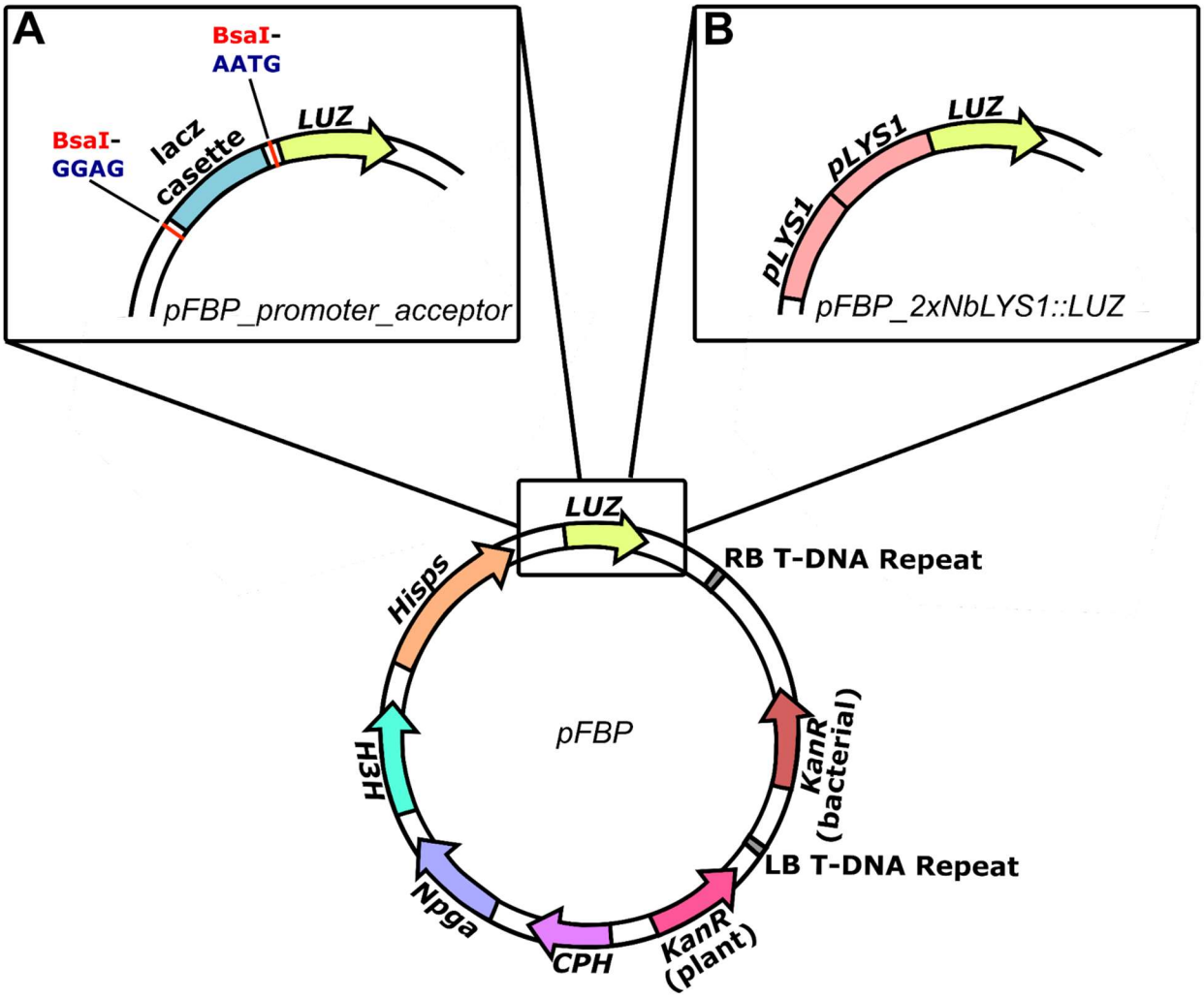

Supplementary Figure S2. A modified FBP construct for rapid cloning and testing of putative promoter regions.

A, The *pFBP_promoter_acceptor* construct contains a *lacz* cassette that allows for blue-white screening to facilitate screening of correct clones. This cassette is flanked by BsaI recognition sites that exposes GGAG and AATG overhangs upon digestion. These overhangs are compatible with MoClo Promoter +5' Untranslated Region Level 0 constructs. B, The *pFBP_2xNbLYS1::LUZ* construct places two identical promoter region sequences of a *N. benthamiana* homolog of *A. thaliana* LYS1 immediately adjacent to the coding sequence of *Neonothopanus nambii LUZ.*

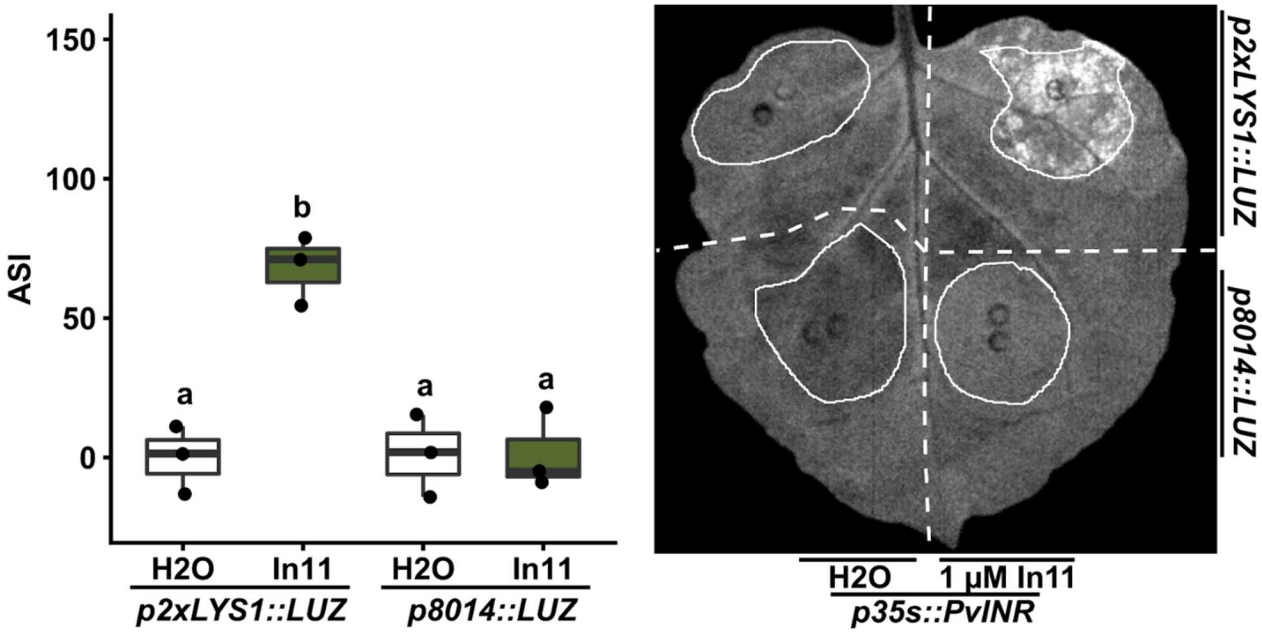

Supplementary Figure S3. The putative promoter region of *Niben101Scf08566g08014* does not serve as a marker of In11 response. We generated *p8014::LUZ,* a construct using the putative promoter region of *Niben101Scf08566g08014* to drive *LUZ* expression. Leaves were coinfiltrated with *35s::PvINR* and *pLYS1::LUZ* across the proximal portion of the leaf, and *35s::PvINR* and *p8014::LUZ* across the distal portion of the leaf. 48 hours after infiltration, one half of the leaf was infiltrated with sterile water, and the other half was infiltrated with 1 µM In11. Images were obtained 6 hours after peptide treatment, and ASI was quantified in ImageJ. Left, boxplots show the average ASI of three independent biological replicates. Letters represent significantly different means (One-way ANOVA and post-hoc Tukey's HSD tests, $p<.05$). Right, a representative leaf image of one biological replicate is depicted.

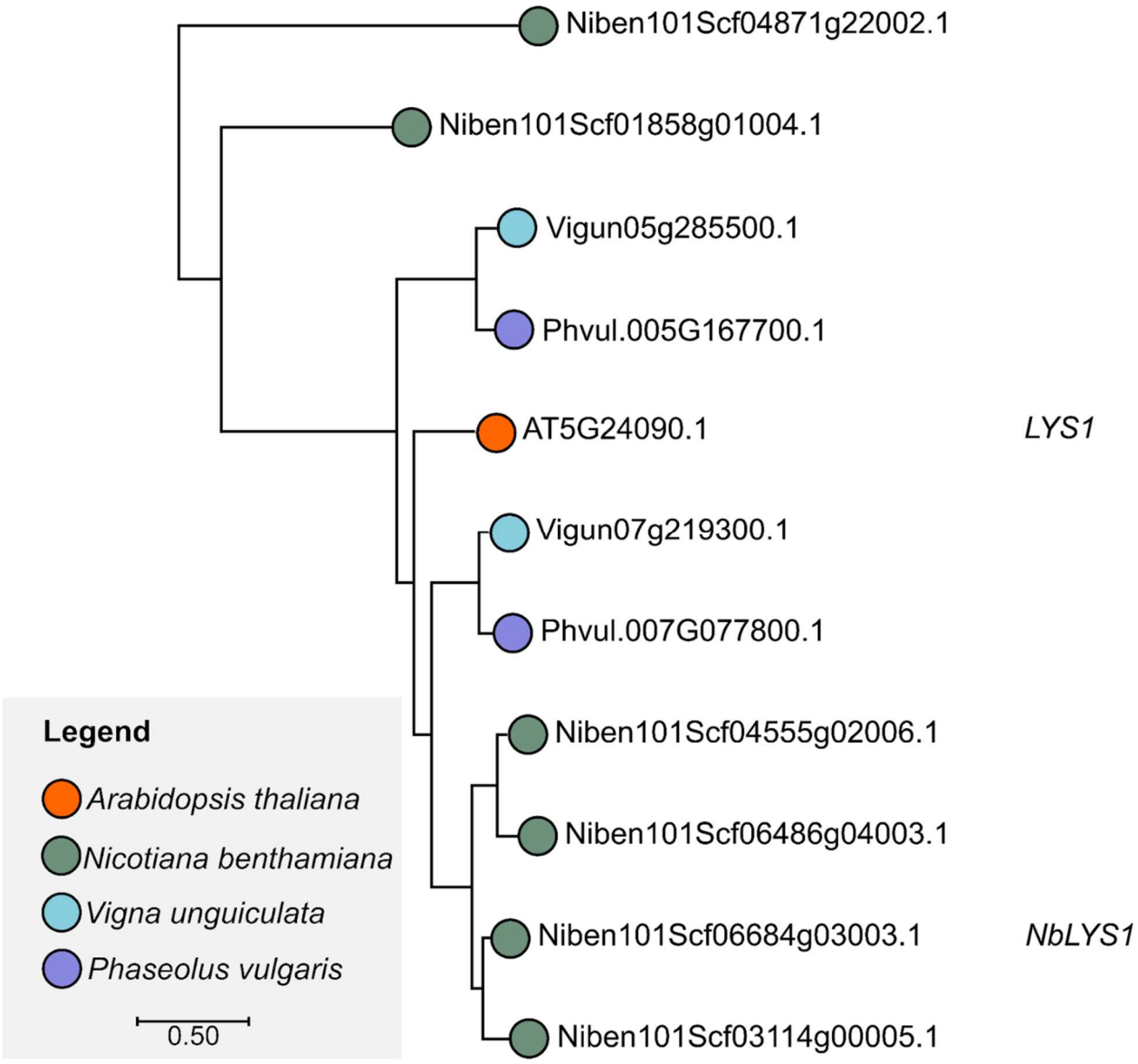

Supplementary Figure S4. The In11-upregulated gene *Niben101Scf06684g03003.1* is a homolog of *A. thaliana LYS1*. A maximum likelihood tree generated from BLASTN results of the *Niben101Scf06684g03003.1* gene indicates close homology to the characterized *Arabidopsis thaliana LYS1* gene.

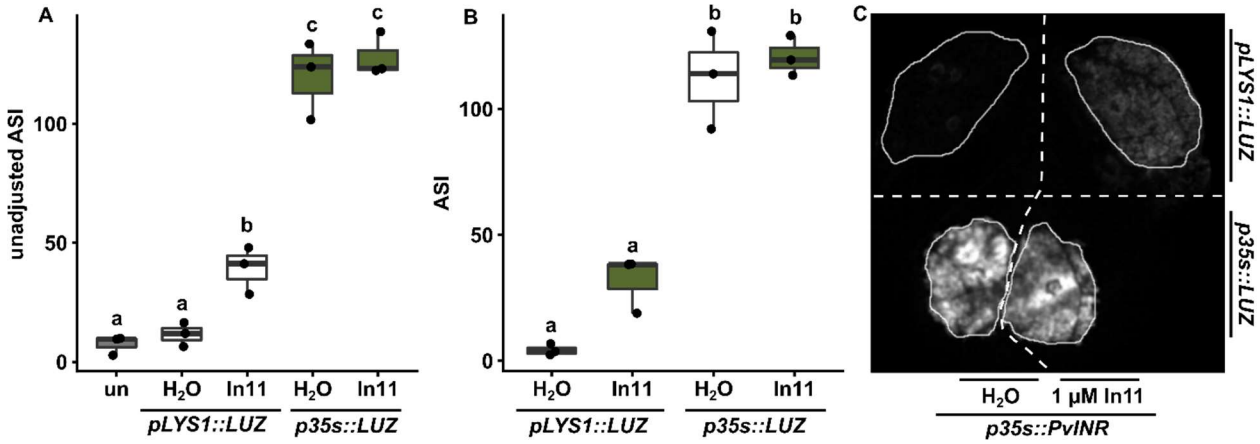

Supplementary Figure S5. The *LYS1* Promoter Drives *LUZ* weaker than the strong constitutive *CaMV35s* promoter. *N. benthamiana* leaves were infiltrated with *p35s::PvINR* and *pLYS1::LUZ* across the proximal portion of the leaf, and *p35s::PvINR* and *p35s::LUZ* across the distal portion of the leaf. 48 hpi, each half of the leaf was infiltrated with either water of 1µM In11. Images were obtained 6 hours after peptide treatment, and average signal intensity (ASI) was quantified using ImageJ. One-way ANOVA and post-hoc Tukey's HSD tests were conducted and summarized as a compact letter display. Statistically significant differences ($p < .05$) among pairwise comparisons are represented by differing letters. A, Unadjusted ASI demonstrates insignificant difference in luminescence produced upon water treatment compared to untransformed and uninfiltrated plant tissue (un). B, Adjusted ASI over three biological replicates reveals relative strengths of expression by the PAMP responsive *NbLYS1* promoter and the strong constitutive *CaMV35s* promoter. C, A representative leaf is shown.